arXiv:0902.4164v1 [hep-ph] 24 Feb 2009

The flavor-changing bottom and anti-strange quark production in the littlest Higgs model with T parity at the ILC

Xuelei Wang,* Jinzhong Han, Wujun Li, and Hao Wang

College of Physics and Information Engineering,
Henan Normal University, Xinxiang, Henan 453007. P.R. China

(Dated: February 24, 2009)

Abstract

Due to the new source of flavor changing(FC) couplings in some new physics models, the production rates of FC processes can be greatly enhanced in these new physics models and some FC processes might be observable. So the FC processes open an ideal window to probe new physics due to their clean SM backgrounds. In this paper, we study some bottom and anti-strange production processes at the ILC in the littlest Higgs model with T-parity(LHT), i.e., $e^+e^- \to b\bar{s}$ and $\gamma\gamma \to b\bar{s}$. In the LHT model mirror quarks induce some new FC couplings and the cross sections are sensitive to the mirror quark masses. With large mirror quark masses, the cross sections can be large enough to make the processes observable. If these FC processes are observed at the ILC, one can obtain up-limit of mirror quark masses.

PACS numbers: 14.65.Ha,12.60.-i, 12.15.Mn,13.85.Lg

---

*Electronic address: wangxuelei@sina.com

I. INTRODUCTION

The Standard Model(SM) suffers from shortcomings, such as the hierarchy problem, Little Higgs model offers an alternative route to solve this problem[1]. The littlest Higgs(LH) model is the most economical implementation of the little Higgs idea[2], but is found to be subject to strong constraints from electroweak precision tests[3]. To solve this problem, one of the most attractive models is proposed which is just the littlest Higgs model with T-parity(LHT)[4], where the discrete symmetry forbids tree-level corrections to electroweak observables, thus weakening the electroweak precision constraints. In this model, the flavor structure is richer than the one of the SM, mainly due to the presence of three doublets of mirror quarks and three doublets of mirror leptons and their weak interactions with the ordinary quarks and leptons. Such new flavor-changing(FC) interactions can have crucial phenomenology. One of the most important phenomenologies is the FC processes induced by the FC interactions in the LHT model. As we know, the SM does not contain the tree-level FC neutral currents, though it can occur at higher order through radiative corrections. Because of the loop suppression, these SM FC effects are hardly observable. The new FC interactions in the LHT model can significantly enhance the FC processes which maybe make some FC processes observable. So the FC processes can open an ideal window to probe the LHT model.

The impact of the FC interactions in the LHT model on the K, B and D systems has been firstly explored in the paper[5], and found constraints on the mirror fermion mass spectrum from a one-loop analysis of neutral meson mixing in the K, B and D systems, following by series of extensive studies of FC transitions in the LHT model[6, 7, 8, 9, 10]. Specially, the group of Blanke et al have extended the analysis of Ref.[6] to included all prominent rare K and B decays and a collection of Feynman rules including v^2/f^2 contributions is given for the first time[7]. The FC interactions in the LHT model can also induce the loop-level $t\bar{c}V(V=\gamma,Z,g)$ and $b\bar{s}V$ couplings. The $t\bar{c}V$ can contribute to the rare top quark decays $t\rightarrow cV$[11] and some FC production processes $eq\rightarrow et$[12], $e^+e^-(\gamma\gamma)\rightarrow t\bar{c}$[13], $pp\rightarrow t\bar{c}(tV)$[14]. On the other hand, the paper[15] has performed a collective study for the various FC decays of B-bosons, Z-boson and Higgs boson, and found that the LHT predictions significantly deviate from the SM predictions. With the FC interactions $b\bar{s}\gamma(Z)$, $b\bar{s}$ can be produced via e^+e^- or $\gamma\gamma$ collision, and in this paper we study this FC $b\bar{s}$ production at the International Linear Collider(ILC).

The International Linear Collider(ILC) with the center of mass(c.m.) energy $\sqrt{s}$=300 GeV-1.5 TeV and the yearly luminosity 500 fb^{-1} has been planned[16]. Due to its rather clean environment and high luminosity, the ILC will be an ideal machine to probe new physics. In such a collider, in addition to e^+e^- collision, one can also realize photon-photon collision. One might observe the clue of the LHT model and study the properties of FC interactions via these FC processes at the ILC.

This paper is organized as follows. In Sec.II, we briefly review the LHT model. Sec.III presents the detailed calculation of the production cross sections of the processes. The numerical results are shown in Sec.IV. We present conclusions in Sec.V

II. A BRIEF REVIEW OF THE LHT MODEL

A detailed description of the LHT model can be found for instance in [5, 6], and here we just want to briefly review the flavor structure of the LHT model and the content related to our calculation.

The LHT model is based on a non-linear sigma model describing the spontaneous breaking of a global $SU(5)$ down to a global $SO(5)$. This symmetry breaking takes place at the scale $f \sim \mathcal{O}(TeV)$. From the $SU(5)/SO(5)$ breaking, there arise 14 Goldstone bosons which are described by the "pion" matrix Π, given explicitly by

$$\Pi = \begin{pmatrix} -\frac{\omega^0}{2} - \frac{\eta}{\sqrt{20}} & -\frac{\omega^+}{\sqrt{2}} & -i\frac{\pi^+}{\sqrt{2}} & -i\phi^{++} & -i\frac{\phi^+}{\sqrt{2}} \\ -\frac{\omega^-}{\sqrt{2}} & \frac{\omega^0}{2} - \frac{\eta}{\sqrt{20}} & \frac{v+h+i\pi^0}{2} & -i\frac{\phi^+}{\sqrt{2}} & \frac{-i\phi^0+\phi^P}{\sqrt{2}} \\ i\frac{\pi^-}{\sqrt{2}} & \frac{v+h-i\pi^0}{2} & \sqrt{4/5}\eta & -i\frac{\pi^+}{\sqrt{2}} & \frac{v+h+i\pi^0}{2} \\ i\phi^{--} & i\frac{\phi^-}{\sqrt{2}} & i\frac{\pi^-}{\sqrt{2}} & -\frac{\omega^0}{2} - \frac{\eta}{\sqrt{20}} & -\frac{\omega^-}{\sqrt{2}} \\ i\frac{\phi^-}{\sqrt{2}} & \frac{i\phi^0+\phi^P}{\sqrt{2}} & \frac{v+h-i\pi^0}{2} & -\frac{\omega^+}{\sqrt{2}} & \frac{\omega^0}{2} - \frac{\eta}{\sqrt{20}} \end{pmatrix} \tag{1}$$

Here, $H = (-i\pi^+\sqrt{2}, (v+h+i\pi^0)/2)^T$ plays the role of the SM Higgs doublet, i.e. h is the usual Higgs field, $v = 246$ GeV is the Higgs VEV, and $\pi^\pm, \pi^0$ are the Goldstone bosons associated with the spontaneous symmetry breaking $SU(2)_L \times U(1)_Y \rightarrow U(1)_{em}$. The fields η and ω are additional Goldstone bosons eaten by heavy gauge bosons when the $[SU(2) \times U(1)]^2$gauge group is broken down to $SU(2)_L \times U(1)_Y$. The field Φ is a physical scalar triplet with

$$\Phi = \begin{pmatrix} -i\phi^{++} & -i\frac{\phi^+}{\sqrt{2}} \\ -i\frac{\phi^+}{\sqrt{2}} & \frac{-i\phi^0+\phi^P}{\sqrt{2}} \end{pmatrix} \tag{2}$$

In the LHT model, a T-parity discrete symmetry is introduced to make the model consistent with the electroweak precision data. Under the T-parity, the fields Φ, ω, and η are odd, and the SM Higgs doublet H is even. The Goldstones ω, and η are present in our analysis.

In the gauge sector, T-parity is realized by the automorphism $T^\alpha \rightarrow T^\alpha$ and $X^\alpha \rightarrow -X^\alpha$. As a result, T-parity interchangings the two sets of gauge bosons,

$$W_1^\alpha \leftrightarrow W_2^\alpha, \qquad B_1 \leftrightarrow B_2. \tag{3}$$

T-parity requires the two sets of gauge couplings to be identical: $g_1 = g_2 = \sqrt{2}g$ and $g_1^{'} = g_2^{'} = \sqrt{2}g^{'}$. The gauge bosons form a light and a heavy linear combination:

$$W_L^\alpha = \frac{1}{\sqrt{2}}(W_1^\alpha + W_2^\alpha), \qquad B_L = \frac{1}{\sqrt{2}}(B_1 + B_2), \qquad (T - even) \tag{4}$$

with masses from usual electroweak symmetry breaking, and

$$W_H^\alpha = \frac{1}{\sqrt{2}}(W_1^\alpha - W_2^\alpha), \qquad B_H = \frac{1}{\sqrt{2}}(B_1 - B_2), \qquad (T - odd) \tag{5}$$

with masses of order f generated from the non-linear sigma model. After electroweak symmetry breaking, the light gauge bosons mix to form the usual physical states of the

SM, $A_L = c_w B_L - s_w W_L^3$, $Z_L = s_w B_L + c_w W_L^3 (c_w = cos\theta_w, s_w = sin\theta_w, \theta_w$ is Weinberg angle)and $W_L^{\pm} = (W_L^1 \mp W_L^2)/\sqrt{2}$. Similarly, through electroweak symmetry breaking, neutral components of W_H^a and B_H are mixed and form mass eigenstates A_H and Z_H. The masses of the heavy bosons are obtained as

$$M_{W_H^{\pm}} = M_{Z_H} = gf, \qquad M_{AH} = \frac{g'}{\sqrt{5}} f \tag{6}$$

The A_H is always lighter than the other T-odd gauge bosons and thus a good candidate for the lightest T-odd particle and dark matter.

A consistent and phenomenologically viable implementation of T-parity in the fermion sector requires the introduction of mirror fermion. T-even fermion section consists of the SM quarks, leptons and an additional heavy quark T_+. The T-odd fermion sector consists of three generations of mirror quarks and leptons and an additional heavy quark T_-. Only the mirror quarks (u_H^i, d_H^i) are involved in this paper. The mirror fermions get masses

$$\begin{aligned} m_{H_i}^u &= \sqrt{2}\kappa_i f(1 - \frac{v^2}{8f^2}) \equiv m_{H_i}(1 - \frac{v^2}{8f^2}), \\ m_{H_i}^d &= \sqrt{2}\kappa_i f \equiv m_{H_i}, \end{aligned} \tag{7}$$

where the Yukawa couplings κ_i can in general depend on the fermion species i.

In this paper only mirror quarks are relevant. We will denote them by

$$\begin{pmatrix} u_H^1 \\ d_H^1 \end{pmatrix}, \quad \begin{pmatrix} u_H^2 \\ d_H^2 \end{pmatrix}, \quad \begin{pmatrix} u_H^3 \\ d_H^3 \end{pmatrix}. \tag{8}$$

with their masses satisfying to first order in v/f

$$m_{uH}^1 = m_{dH}^1, \qquad m_{uH}^2 = m_{dH}^2, \qquad m_{uH}^3 = m_{dH}^3. \tag{9}$$

The mirror fermions induce a new flavor structure and there are four CKM-like unitary mixing matrices in the mirror fermion sector:

$$V_{H_u}, \quad V_{H_d}, \quad V_{H_l}, \quad V_{H_\nu}. \tag{10}$$

In the course of our analysis it will be useful to introduce the following quantities:

$$\xi_i^{(k)} = V_{Hd}^{*is} V_{Hd}^{id}, \qquad \xi_i^{(d)} = V_{Hd}^{*ib} V_{Hd}^{id}, \qquad \xi_i^{(s)} = V_{Hd}^{*ib} V_{Hd}^{is}, \qquad (i = 1, 2, 3), \tag{11}$$

The V_{H_d} is parameterized with three angles $\theta_{12}^d, \theta_{23}^d, \theta_{13}^d$ and three phases $\delta_{12}^d, \delta_{23}^d, \delta_{13}^d$

$$V_{H_d} = \begin{pmatrix} c_{12}^d c_{13}^d & s_{12}^d c_{13}^d e^{-i\delta_{12}^d} & s_{13}^d e^{-i\delta_{13}^d} \\ -s_{12}^d c_{23}^d e^{i\delta_{12}^d} - c_{12}^d s_{23}^d s_{13}^d e^{i(\delta_{13}^d - \delta_{23}^d)} & c_{12}^d c_{23}^d - s_{12}^d s_{23}^d s_{13}^d e^{i(\delta_{13}^d - \delta_{12}^d - \delta_{23}^d)} & s_{23}^d c_{13}^d e^{-i\delta_{23}^d} \\ s_{12}^d s_{23}^d e^{i(\delta_{12}^d + \delta_{23}^d)} - c_{12}^d c_{23}^d s_{13}^d e^{i\delta_{13}^d} & -c_{12}^d s_{23}^d e^{i\delta_{23}^d} - s_{12}^d c_{23}^d s_{13}^d e^{i(\delta_{13}^d - \delta_{12}^d)} & c_{23}^d c_{13}^d \end{pmatrix} \tag{12}$$

III. THE BOTTOM AND ANTI-STRANGE QUARK PRODUCTION IN THE LHT MODEL AT THE ILC

We have mentioned that there are FC interactions between SM fermions and T-odd mirror fermions which are mediated by the T-odd heavy gauge bosons($A_H, Z_H, W_H^{\pm}$) or Goldstone bosons($\eta, \omega^0, \omega^{\pm}$). The relevant Feynman rules can be found in Ref.[7]. With these FC couplings, the loop-level FC couplings $b\bar{s}Z(\gamma)$ can be induced and the relevant Feynman diagrams are shown in Fig.1. As we know, each diagram in Fig.1 actually contains ultraviolet divergence. Because there is no corresponding tree-level $b\bar{s}Z(\gamma)$ couplings to absorb these divergences, the divergences just cancel each other and the total effective $b\bar{s}Z(\gamma)$ couplings are finite as they should be. The effective one loop-level couplings $b\bar{s}Z(\gamma)$ can be directly calculated based on Fig.1. Here we use the method introduced in Ref.[17] to obtain the effective vertex $b\bar{s}Z(\gamma)$ firstly. Such method can greatly simplify our calculations since it avoids repetition of the evaluation of a same loop-corrected vertex in different places, or in different processes. Their explicit forms, $\Gamma^{\mu}_{b\bar{s}\gamma}(p_b, p_{\bar{s}})$ and $\Gamma^{\mu}_{b\bar{s}Z}(p_b, p_{\bar{s}})$, are given in Appendix A. The study has shown that the FC couplings $b\bar{s}Z$ can largely enhance the branching ratios of rare Z boson decay $Z \to b\bar{s}$[15]. On the other hand, the FC couplings $b\bar{s}Z(\gamma)$ can also contribute to the $b\bar{s}$ production via the processes $e^+e^-(\gamma\gamma) \to b\bar{s}$. We will discuss these processes in the following.

A. The production amplitudes of the process $e^+e^- \to b\bar{s}$

In the LHT model, the existence of the FC couplings $b\bar{s}Z(\gamma)$ can induce the process $e^+e^- \to b\bar{s}$ at loop-level via s-channel. The corresponding Feynman diagram is shown in Fig.2(A). The production amplitudes are

$$M_A = M_A^{\gamma} + M_A^{Z},$$

with

$$M_A^{\gamma} = -eG(p_1 + p_2, 0)\bar{u_b}(p_3)\Gamma^u_{b\bar{s}\gamma}(p_3, p_4)v_{\bar{s}}(p_4)\bar{v}_{e^+}(p_2)\gamma_u u_{e^-}(p_1), \tag{13}$$

$$\begin{aligned} M_A^Z \;=\; & \frac{g}{c_w}G(p_1 + p_2, M_Z)\bar{u_b}(p_3)\Gamma^u_{bsZ}(p_3, p_4)v_{\bar{s}}(p_4)\bar{v}_{e^+}(p_2)\gamma_u \\ & \times[(-\frac{1}{2} + s_w^2)P_L + s_w^2 P_R]u_{e^-}(p_1). \end{aligned} \tag{14}$$

Where $P_L = \frac{1}{2}(1-\gamma_5)$ and $P_R = \frac{1}{2}(1+\gamma_5)$ are the left and right chirality projectors. p_1, p_2 are the momenta of the incoming e^+, e^-, and p_3, p_4 are the momenta of the outgoing final states bottom quark and anti-strange quark, respectively. We also define $G(p, m)$ as $\frac{1}{p^2-m^2}$.

B. The production amplitudes of the process $\gamma\gamma \to b\bar{s}$

On the other hand, a unique feature of the ILC is that it can be transformed to $\gamma\gamma$ collision with the photon beams generated by using the Compton backscattering of the initial electron and laser beams. In this case, the energy and luminosity of the photon beams would be the same order of magnitude of the original electron beams, and the set of final states at a photon collider is much richer than that in the e^+e^- mode. In the LHT model, $b\bar{s}$ can also be produced through $\gamma\gamma$ collision. The process $\gamma\gamma \to b\bar{s}$ has some advantages in probing new physics. Firstly, unlike the process $e^+e^- \to b\bar{s}$, which is induced by s-channel and its production rate is suppressed in high energy collisions, there are $t-$ and $u-$channel contributions to $\gamma\gamma \to b\bar{s}$ and thus its cross section may be much larger at the ILC. Secondly, the process $\gamma\gamma \to b\bar{s}$ is essentially free from any SM irreducible background. So the realization of the photon collider will open a wider window to probe new physics. The relevant Feynman diagrams of $\gamma\gamma \to b\bar{s}$ in the LHT model are shown in Fig.2(B-C). The invariant production amplitudes of the process $\gamma\gamma \to b\bar{s}$ can be written as:

$$M_B = \frac{1}{3}eG(p_3 - p_1, m_s)\bar{u}_b(p_3)\Gamma^{\mu}_{b\bar{s}\gamma}(p_3, p_1 - p_3)\epsilon_\mu(p_1)(\not{p}_3 - \not{p}_1 + m_s)\not{\epsilon}(p_2)\nu_{\bar{s}}(p_4), \quad (15)$$

$$M_C = \frac{1}{3}eG(p_2 - p_4, m_b)\bar{u}_b(p_3)\not{\epsilon}(p_1)(\not{p}_2 - \not{p}_4 + m_b)\Gamma^{\mu}_{b\bar{s}\gamma}(p_2 - p_4, p_4)\epsilon_\mu(p_2)\nu_{\bar{s}}(p_4). \quad (16)$$

With the above amplitudes $M_B,\ M_C$, we can directly obtain the production cross section $\hat{\sigma}(\hat{s})$ for the subprocess $\gamma\gamma \to b\bar{s}$ and the total cross sections at the e^+e^- linear collider can be obtained by folding $\hat{\sigma}(\hat{s})$ with the photon distribution function $F(x)$ which is given in Ref.[18],

$$\sigma_{tot}(s) = \int_{x_{min}}^{x_{max}} dx_1 \int_{x_{min}x_{max}/x_1}^{x_{max}} dx_2 F(x_1)F(x_2)\hat{\sigma}(\hat{s}), \quad (17)$$

where s is the c.m. energy squared for e^+e^-. The subprocess occurs effectively at $\hat{s} = x_1 x_2 s$, and x_i are the fractions of the electron energies carried by the photons. The explicit form of the photon distribution function $F(x)$ is

$$F(x) = \frac{1}{D(\xi)}\left[1 - x + \frac{1}{1-x} - \frac{4x}{\xi(1-x)} + \frac{4x^2}{\xi^2(1-x)^2}\right], \quad (18)$$

with

$$D(\xi) = \left(1 - \frac{4}{\xi} - \frac{8}{\xi^2}\right)\ln(1+\xi) + \frac{1}{2} + \frac{8}{\xi} - \frac{1}{2(1+\xi)^2}, \quad (19)$$

and

$$\xi = \frac{4E_0\omega_0}{m_e^2}. \quad (20)$$

E_0 and ω_0 are the incident electron and laser light energies, and $x = \omega/E_0$. The energy ω of the scattered photon depends on its angle θ with respect to the incident electron beam and is given by

$$\omega = \frac{E_0(\frac{\xi}{1+\xi})}{1 + (\frac{\theta}{\theta_0})^2}. \quad (21)$$

Therefore, at $\theta = 0$, $\omega = E_0\xi/(1+\xi) = \omega_{max}$ is the maximum energy of the backscattered photon, and $x_{max} = \frac{\omega_{max}}{E_0} = \frac{\xi}{1+\xi}$. To avoid unwanted e^+e^- pair production from the collision between the incident and back-scattered photons, we should not choose too large ω_0. The threshold for e^+e^- pair creation is $\omega_{max}\omega_0 > m_e^2$, so we require $\omega_{max}\omega_0 \le m_e^2$. Solving $\omega_{max}\omega_0 = m_e^2$, we find

$$\xi = 2(1 + \sqrt{2}) = 4.8. \tag{22}$$

For the choice $\xi = 4.8$, we obtain $x_{max} = 0.83$ and $D(\xi_{max}) = 1.8$. The minimum value for x is determined by the production threshold

$$x_{min} = \frac{\hat{s}_{min}}{x_{max}s}, \quad \hat{s}_{min} = (m_b + m_s)^2. \tag{23}$$

Here we have assumed that both photon beams and electron beams are unpolarized. We also assume that, the number of the backscattered photons produced per electron is one.

IV. THE NUMERICAL RESULTS OF THE CROSS SECTIONS FOR THE PROCESSES $e^+e^-(\gamma\gamma) \to b\bar{s}$ IN THE LHT MODEL

To obtain numerical results of the cross sections, we calculate the amplitudes numerically by using the method of reference[19], instead of calculating the square of the production amplitudes analytically. This greatly simplifies our calculations. There are several free parameters in the LHT model which are involved in the production amplitudes. They are the breaking scale f, the masses of the mirror quarks $m_{H_i} (i = 1, 2, 3)$(Here we have ignored the masses difference between up-type mirror quarks and down-type mirror quarks), and 6 parameters(θ_{12}^d, θ_{13}^d, θ_{23}^d, δ_{12}^d, δ_{13}^d, δ_{23}^d) which are related to the mixing matrix V_{H_d}. In Ref.[6, 7] the constraints on the mass spectrum of the mirror fermions have been investigated from the analysis of neutral meson mixing in the K, B and D systems. They found that a TeV scale GIM suppression is necessary for a generic choice of V_{H_d}. However, there are regions of parameter space where are only very loose constraints on the mass spectrum of the mirror fermions. Here we study the processes $e^+e^-(\gamma\gamma) \to b\bar{s}$ based on the two scenarios for the structure of the matrix V_{H_d}, as in Ref.[11]. i.e., for case I

$$V_{H_d} = V_{CKM}.$$

For case II, δ_{13}^d is a free parameter, while other parameters in the matrix V_{Hd} are assumed as

$$\delta_{12}^d = \delta_{23}^d = 0, \frac{1}{\sqrt{2}} \le s_{12}^d \le 0.99, \quad 5 \times 10^{-5} \le s_{23}^d \le 2 \times 10^{-4}, \quad 4 \times 10^{-2} \le s_{13}^d \le 0.6.$$

To fix matrix V_{Hd} in Case II, we adopt the upper limit and down limit of s_{ij}^d, respectively,

$$CaseII(1): \quad \delta_{12}^d = \delta_{13}^d = \delta_{23}^d = 0, s_{12}^d = \frac{1}{\sqrt{2}}, s_{23}^d = 5 \times 10^{-5}, s_{13}^d = 4 \times 10^{-2},$$

$$CaseII(2): \quad \delta_{12}^d = \delta_{13}^d = \delta_{23}^d = 0, s_{12}^d = 0.99, s_{23}^d = 2 \times 10^{-4}, s_{13}^d = 0.6.$$

In both cases, the constraints on the mass spectrum of the mirror fermions are very relaxed. On the other hand, the Ref.[20] has shown that the experimental bounds on four-fermi interactions involving SM fields provide an upper bound on the mirror fermion masses and this yields $m_{H_i} \leq 4.8f^2$. In our calculation, we also consider such constraint. For the breaking scale f, we take two typical values: 500 GeV and 1000 GeV. To get the numerical results of the cross sections, we should also fix some parameters in the SM as m_b =4.7 GeV, m_s =0.095 GeV, s_w^2 =0.23, M_Z =91.87 GeV, $\alpha_e = 1/128$, and $v = 246$ GeV[21]. For the c.m. energies of the ILC, we choose $\sqrt{s} = 500,\ 1000$ GeV as examples. On the other hand, taking account of the detector acceptance, we have taken the basic cuts on the transverse momentum(p_T) and the pseudo-rapidity(η) for the final state particles

$$p_T \geq 20GeV, \qquad |\eta| \leq 2.5.$$

The numerical results of the cross sections are summarized in Figs.3-5, and the anti-bottom production is also included in our calculation. In Figs.3-5, we plot the cross sections of the processes $e^+e^-(\gamma\gamma) \to b\bar{s}$ as a function of M_{H_3} for case I and case II, respectively. In case I, the mixing in the up type gauge and Goldstone boson interactions is absent. In this case there are no constraints on the masses of the mirror quarks at one loop-level from the K and B systems and the constraints come only from the D system. The constraints on the mass of the third generation mirror quark are very weak. Here the other constraint $m_{H_i} \leq 4.8f^2$ should also be considered. So we take m_{H_3} to vary in the range of $500 - 1200$ GeV for $f = 500$ GeV and $500 - 4800$ GeV for $f = 1000$ GeV, and fix $m_{H_1} = m_{H_2}$=500 GeV. We can see from Fig.3 that both cross sections of the processes $e^+e^- \to b\bar{s}$ and $\gamma\gamma \to b\bar{s}$ rise very fast with the m_{H_3} increasing. This is because the couplings between the mirror quarks and the SM quarks are proportional to the masses of the mirror quarks. The masses of the heavy gauge bosons and the mirror quarks, M_{V_H} and m_{H_i}, are proportional to f, but the cross sections of both processes are insensitive to the scale f because the production amplitudes are represented in the form of m_{H_i}/M_{V_H}. For Case II(1) and Case II(2), the dependence of the cross sections on m_{H_3} is presented in Fig.4-5. In this case, the constraints from the K and B systems are also very weak. Compared to Case I, the mixing between the second and third generations is enhanced with the choice of a bigger mixing angle s_{23}^d. Even with stricter constraints on the masses of the mirror quarks, the large masses of the mirror quarks can also enhance the cross sections significantly. The dependence of the cross sections on m_{H_3} is similar to that in Case I. In both Case I and case II, the cross section of $\gamma\gamma \to b\bar{s}$ is several orders of magnitude larger than that of $e^+e^- \to b\bar{s}$. So the process $\gamma\gamma \to b\bar{s}$ benefits from a large cross section. In order to provide more information for ILC experiments to probe the LHT model via the $b\bar{s}$ production, we also give out the transverse momentum distributions of the bottom quark in Fig.6. We fix $\sqrt{s} = 500$ GeV, $f = 500$ GeV, $m_{H_1} = m_{H_2} = m_{H_3} = 1000$ GeV for both Case I and Case II. We can see that the p_b^T distributions of two processes are very different. The p_b^T distribution of the process $e^+e^- \to b\bar{s}$ increases with p_b^T increasing, but the p_b^T distribution of the process $\gamma\gamma \to b\bar{s}$ decreases sharply with p_b^T. These two processes can provide complementary information in different transverse momentum space.

V. CONCLUSIONS AND SUMMARIES

In this paper, we study two FC $b\bar{s}$ production processes in the LHT model at the ILC, i.e., $e^+e^- \to b\bar{s}$ and $\gamma\gamma \to b\bar{s}$. There exist some new sources of FC couplings in the LHT model, so the cross sections of these processes are significantly enhanced. The cross sections are sensitive to the mirror quark masses very much and the large mirror quark masses can enhance the cross sections to the observable level of ILC experiments.

VI. ACKNOWLEDGMENTS

This work is supported by the National Natural Science Foundation of China under Grant No.10775039.

---

[1] N. Arkani-Hamed, A. G. Cohen and H. Georgi, *Phys. Lett.* B**513**, 232(2001).

[2] N. Arkani-Hamed, A. G. Cohen, E. Katz, A. E. Nelson, *JHEP* **0207**, 034(2002).

[3] J. L. Hewett, F. J. Petriello, and T. G. Rizzo, *JHEP* **0310**, 062(2003); C. Csaki, J. Hubisz, G. D. Kribs, P. Meade, and J. Terning, *Phys.Rev.* D**67**, 115002(2003).

[4] I. Low, *JHEP*, **0410**, 067(2004); H. C. Cheng and I. Low, *JHEP*, **0408**, 061(2004); J. Hubisz and P.Meade, *Phys.Rev.* D**71**, 035016(2005); J. Hubisz, S. J. Lee and G. Paz, *JHEP*, **0606**, 041(2006).

[5] J. Hubisz, S. J. Lee, and G. Paz, *JHEP* **0606**, 041(2006).

[6] M. Blanke, A. J. Buras, A. Poschenrieder, C. Tarantino, S. Uhlig and A. Weiler, *JHEP* **0612**, 003(2006).

[7] M. Blanke, A. J. Buras, A. Poschenrieder, S. Recksiegel, C. Tarantino, S. Uhlig and A. Weiler, *JHEP* **0701**, 066(2007).

[8] M. Blanke, A. J. Buras, S. Recksiegel, C. Tarantino, S. Uhlig, *Phys.Lett.* B**657**, 81(2007).

[9] M.Blanke, A.J.Buras, S.Recksiegel, C.Tarantino and S.Uhlig, *JHEP* **0706**, 082(2007).

[10] M. Blanke, A. J. Buras, B. Duling, A. Poschenrieder, C. Tarantino, *JHEP* **0705**, 013(2007); S. R. Choudhury, A. S. Cornell, A. Deandrea, N. Gaur, A. Goyal, hep-ph/0612327.

[11] H. S. Hou, hep-ph/0703067.

[12] C. X. Yue, J. Wen, J. Y. Liu, W. Liu, hep-ph/08031335.

[13] Xuelei Wang, Huiling Jin, Yanju Zhang, Yanhui Xi, *Nucl.Phys.* B**807**, 210(2009).

[14] Xuelei Wang, Yanju Zhang, Huiling Jin, Yanhui Xi, *Nucl.Phys.* B**810**, 226(2009).

[15] Xiao-Fang Han, Lei Wang, Jinmin Yang, hep-ph/0807.4480.

[16] T. Abe *et al.*[American Linear Collider Group], hep-ex/0106057; J. A. Aguilar-Saavedra *et al.*[ECFA/DESY LC Physics Working Group], hep-ph/0106315; K. Abe *et al.*[ACFA Linear Collider Working Group], hep-ph/0109166; G. Laow *et al.*, ILC Techinical Review Committee, second report, 2003, SLAC-R-606.

[17] J. J. Cao, G. Eilam, M.Frank, K. Hikasa, G. L. Liu, I. Turan, and J. M. Yang, *Phys. Rev.* D**75**, 075021(2007).

[18] G. Jikia, *Nucl. Phys.* B**374**, 83(1992); O. J. P. Eboli, et al., *Phys. Rev.* D**47**, 1889(1993); K. M. Cheung, *ibid.* **47**, 3750 (1993).

[19] K. Hagiwara and D. Zeppenfeld, *Nucl. Phys.* B**313**, 560(1989); V. Barger, T. Han and D. Zeppenfeld, *Phys. Rev.* D**41**, 2782(1990).

[20] J. Hubisz, P. Meade, A. Noble, M. Perelstein, *JHEP* **0601**, 135(2006).

[21] Particle Data Group, W. -M. Yao *et al.*, *J.Phys.* G**33** 1(2006).

[22] M. Clements et al., *Phys. Rev.* D**27**, 570(1983); A. Axelrod, *Nucl. Phys.* B**209**, 349(1982); G. Passarino and M. Veltman, *Nucl. Phys.* B**160**, 151(1979).

Appendix A: The explicit expressions of the effective $b\bar{s}Z(\gamma)$ couplings $\Gamma^{\mu}_{b\bar{s}\gamma}$, $\Gamma^{\mu}_{b\bar{s}Z}$

The effective $b\bar{s}Z(\gamma)$ couplings $\Gamma^{\mu}_{b\bar{s}\gamma}$, $\Gamma^{\mu}_{b\bar{s}Z}$ can be directly calculated based on Fig.1, and they can be represented in form of 2-point and 3-point standard functions B_0, B_1, C_{ij}. In our calculation, the high order $1/f^2$ terms in the masses of new gauge bosons and in the Feynman rules are ignored. $\Gamma^{\mu}_{b\bar{s}\gamma}$ and $\Gamma^{\mu}_{b\bar{s}Z}$ depend on the momenta of bottom quark and anti-strange quark $(p_b, p_{\bar{s}})$. Here p_b and $p_{\bar{s}}$ are both outgoing momenta. The explicit expressions of $\Gamma^{\mu}_{b\bar{s}\gamma}$, $\Gamma^{\mu}_{b\bar{s}Z}$ are

$$\begin{aligned}\Gamma^{\mu}_{b\bar{s}\gamma}(p_b, p_{\bar{s}}) \ = \ & \Gamma^{\mu}_{b\bar{s}\gamma}(\eta^0) + \Gamma^{\mu}_{b\bar{s}\gamma}(\omega^0) + \Gamma^{\mu}_{b\bar{s}\gamma}(\omega^{\pm}) + \Gamma^{\mu}_{b\bar{s}\gamma}(A_H) + \Gamma^{\mu}_{b\bar{s}\gamma}(Z_H) + \Gamma^{\mu}_{b\bar{s}\gamma}(W_H^{\pm}) \\ & + \Gamma^{\mu}_{b\bar{s}\gamma}(W_H^{\pm}\omega^{\pm}),\end{aligned}$$

$$\begin{aligned}\Gamma^{\mu}_{b\bar{s}\gamma}(\eta^0) \ = \ & \frac{i}{16\pi^2}\frac{eg'^2}{300M^2_{A_H}}(V_{Hd})^*_{ib}(V_{Hd})_{is}A \\ & A = [\frac{m_b^2}{m_b^2 - m_s^2}(m_{Hi}^2 B_0(-p_b, m_{Hi}, 0) - m_{Hi}^2 B_0(-p_{\bar{s}}, m_{Hi}, 0) \\ & + m_{Hi}^2 B_1(-p_b, m_{Hi}, 0) - m_s^2 B_1(-p_{\bar{s}}, m_{Hi}, 0)) + \frac{m_s^2}{m_b^2 - m_s^2}(m_{Hi}^2 B_0(-p_b, m_{Hi}, 0) \\ & - m_{Hi}^2 B_0(-p_{\bar{s}}, m_{Hi}, 0) + m_b^2 B_1(-p_b, m_{Hi}, 0) - m_{Hi}^2 B_1(-p_{\bar{s}}, m_{Hi}, 0)) \\ & + m_{Hi}^2(m_b^2(C_{21}^a + C_{11}^a + C_0^a) + m_s^2(C_{22}^a + C_{12}^a + C_0^a) + 2p_b\cdot p_{\bar{s}}(C_{23}^a + C_{12}^a) \\ & + 2C_{24}^a - m_{Hi}^2 C_0^a) + m_s^2 m_b^2(C_{11}^a - C_{12}^a)]\gamma^{\mu}P_L + [\frac{m_b m_s}{m_b^2 - m_s^2}(m_{Hi}^2(2B_0(-p_b, m_{Hi}, 0) \\ & - 2B_0(-p_{\bar{s}}, m_{Hi}, 0) + B_1(-p_b, m_{Hi}, 0) - B_1(-p_{\bar{s}}, m_{Hi}, 0)) + m_b^2 B_1(-p_b, m_{Hi}, 0) \\ & - m_s^2 B_1(-p_{\bar{s}}, m_{Hi}, 0)) + m_{Hi}^2 m_b m_s(C_{11}^a - C_{12}^a + 3C_0^a) + m_b m_s(m_b^2(C_{21}^a + C_{11}^a) \\ & + m_s^2(C_{22}^a + C_{12}^a) + 2p_b\cdot p_{\bar{s}}(C_{23}^a + C_{12}^a) + 2C_{24}^a)]\gamma^{\mu}P_R + [(-2m_{Hi}^2 m_b)(2C_{11}^a \\ & + C_{21}^a + C_0^a) + m_s^2 m_b(C_{23}^a + C_{12}^a)]p_b^{\mu}P_L + [2m_{Hi}^2 m_s(C_{23}^a + C_{12}^a - C_{11}^a - C_0^a) \\ & - 2m_s m_b^2(C_{21}^a + C_{11}^a)]p_b^{\mu}P_R + [-2m_{Hi}^2 m_b(2C_{12}^a + C_{23}^a) + 2m_b m_s^2(C_{12}^a + C_{22}^a)]p_{\bar{s}}^{\mu}P_L \\ & + [2m_{Hi}^2 m_s C_{22}^a - 2m_s m_b^2(C_{12}^a + C_{23}^a)]p_{\bar{s}}^{\mu}P_R,\end{aligned}$$

$$\Gamma^{\mu}_{b\bar{s}\gamma}(\omega^0) \ = \ -\frac{i}{16\pi^2}\frac{eg^2}{12M^2_{Z_H}}(V_{Hd})^*_{ib}(V_{Hd})_{is}B(B = A(C_{ij}^a \rightarrow \ C_{ij}^b, C_0^a \rightarrow \ C_0^b)),$$

$$\begin{aligned}
\Gamma^{\mu}_{b\bar{s}\gamma}(\omega^{\pm}) \;=\; & \frac{i}{16\pi^2}\frac{eg^2}{2M^2_{W_H}}(V_{Hd})^*_{ib}(V_{Hd})_{is} \\
& \times\{[(-\frac{1}{3})(\frac{m_b^2}{m_b^2-m_s^2}(m^2_{Hi}B_0(-p_b,m_{Hi},0)-m^2_{Hi}B_0(-p_{\bar{s}},m_{Hi},0) \\
& +m^2_{Hi}B_1(-p_b,m_{Hi},0)-m_s^2B_1(-p_{\bar{s}},m_{Hi},0)) \\
& +\frac{m_s^2}{m_b^2-m_s^2}(m^2_{Hi}B_0(-p_b,m_{Hi},0)-m^2_{Hi}B_0(-p_{\bar{s}},m_{Hi},0)+m_b^2B_1(-p_b,m_{Hi},0) \\
& -m^2_{Hi}B_1(-p_{\bar{s}},m_{Hi},0))+\frac{2}{3}(m^2_{Hi}(m_b^2(C^c_{21}+C^c_{11}+C^c_0)+m_s^2(C^c_{22}+C^c_{12}+C^c_0) \\
& +2p_b\cdot p_{\bar{s}}(C^c_{23}+C^c_{12})+2C^c_{24}-m^2_{Hi}C^c_0)+m_s^2m_b^2(C^c_{11}-C^c_{12}))-2m^2_{Hi}C^g_{24}]\gamma^{\mu}P_L \\
& +[(-\frac{1}{3})(\frac{m_bm_s}{m_b^2-m_s^2}(m^2_{Hi}(2B_0(-p_b,m_{Hi},0)-2B_0(-p_{\bar{s}},m_{Hi},0) \\
& +B_1(-p_b,m_{Hi},0)-B_1(-p_{\bar{s}},m_{Hi},0))+m_b^2B_1(-p_b,m_{Hi},0) \\
& -m_s^2B_1(-p_{\bar{s}},m_{Hi},0))+\frac{2}{3}(m^2_{Hi}m_bm_s(C^c_{11}-C^c_{12}+3C^c_0)+m_bm_s(m_b^2(C^c_{21} \\
& +C^c_{11})+m_s^2(C^c_{22}+C^c_{12})+2p_b\cdot p_{\bar{s}}(C^c_{23}+C^c_{12})+2C^c_{24}))-2m_bm_sC^g_{24}]\gamma^{\mu}P_R \\
& +[\frac{2}{3}(-2m^2_{Hi}m_b)(2C^c_{11}+C^c_{21}+C^c_0)+2m_s^2m_b(C^c_{23}+C^c_{12})+m_bm_s^2(2C^g_{23} \\
& +C^g_{12})-m_{Hi}m_b(2C^g_{23}+C^g_{12})]p^{\mu}_bP_L+[\frac{2}{3}(2m^2_{Hi}m_s(C^c_{23}+C^c_{12}-C^c_{11}-C^c_0) \\
& -2m_sm_b^2(C^c_{21}+C^c_{11}))+m^2_{Hi}m_s(2C^g_{11}+C^g_0+2C^g_{23}+C^g_{12})-m_b^2m_s(3C^g_{11} \\
& +C^g_0+2C^g_{21})]p^{\mu}_bP_R+[\frac{2}{3}(-2m^2_{Hi}m_b(2C^c_{12}+C^c_{23})+2m_bm_s^2(C^c_{12}+C^c_{22})) \\
& +m_bm_s^2(2C^g_{22}+C^g_{12})-m_{Hi}m_b(2C^g_{23}+C^g_{11})]p^{\mu}_{\bar{s}}P_L+[\frac{2}{3}(2m^2_{Hi}m_sC^c_{22} \\
& -2m_sm_b^2(C^c_{12}+C^c_{23}))+m^2_{Hi}m_s(2C^c_{12}+C^c_0+2C^c_{22}+C^c_{12})-m_b^2m_s(2C^g_{12} \\
& +C^g_0+2C^g_{23}+C^g_{11})]p^{\mu}_{\bar{s}}P_R\},
\end{aligned}$$

$$\begin{aligned}
\Gamma^{\mu}_{b\bar{s}\gamma}(A_H) \;=\; & -\frac{i}{16\pi^2}\frac{eg'^2}{150}(V_{Hd})^*_{ib}(V_{Hd})_{is}C \\
& C=[\frac{m_b^2}{m_b^2-m_s^2}B_1(-p_b,m_{Hi},M_{A_H})-\frac{m_s^2}{m_b^2-m_s^2}B_1(-p_{\bar{s}},m_{Hi},M_{A_H}) \\
& +m_b^2(C^d_{21}+C^d_{11})+m_s^2(C^d_{12}+C^d_{22})+2p_b\cdot p_{\bar{s}}(C^d_{11}+C^d_{23})+2C^d_{24} \\
& -m^2_{Hi}C^d_0]\gamma^{\mu}P_L+[\frac{m_bm_s}{m_b^2-m_s^2}(B_1(-p_b,m_{Hi},M_{A_H})-B_1(-p_{\bar{s}},m_{Hi},M_{A_H})) \\
& +m_bm_s(C^d_{12}-C^d_{11})]\gamma^{\mu}P_R+[-2m_b(C^d_{21}+C^d_{11})]p^{\mu}_bP_L+[2m_s(C^d_{11}+C^d_{23})]p^{\mu}_bP_R \\
& +[-2m_b(C^d_{23}+C^d_{11})]p^{\mu}_{\bar{s}}P_L+[2m_s(C^d_{11}+C^d_{22})]p^{\mu}_{\bar{s}}P_R,
\end{aligned}$$

$$\Gamma^{\mu}_{b\bar{s}\gamma}(Z_H) \;=\; -\frac{i}{16\pi^2}\frac{eg^2}{6}(V_{Hd})^*_{ib}(V_{Hd})_{is}D(D=C(C^d_{ij}\to\; C^e_{ij},C^d_0\to\; C^e_0)),$$

$$\begin{aligned}
\Gamma^{\mu}_{b\bar{s}\gamma}(W^{\pm}_{H}) \;=\;& -\frac{i}{16\pi^2}\frac{eg^2}{3}(V_{Hd})^{*}_{ib}(V_{Hd})_{is} \\
& \times\{[\frac{2m_b^2}{m_b^2-m_s^2}B_1(-p_b,m_{Hi},M_{W_H})-\frac{2m_s^2}{m_b^2-m_s^2}B_1(-p_{\bar{s}},m_{Hi},M_{W_H}) \\
& -4m_b^2(C^f_{21}+C^f_{11})-4m_s^2(C^f_{22}+C^f_{12})-8p_b\cdot p_{\bar{s}}(C^f_{11}+C^f_{23})-8C^f_{24} \\
& +4m^2_{Hi}C^f_0+4C^h_{24}+2B_0(-p_{\bar{s}},m_{Hi},M_{W_H})+2m^2_{WH}C^h_0+m_b^2(3C^h_{11} \\
& +C^h_0)+m_s^2C^h_{12}+4p_b\cdot p_{\bar{s}}(C^h_0+C^h_{11})]\gamma^{\mu}P_L+[\frac{m_bm_s}{m_b^2-m_s^2}(B_1(-p_b,m_{Hi},M_{W_H}) \\
& -B_1(-p_{\bar{s}},m_{Hi},M_{W_H}))-4m_bm_s(C^f_{12}-C^f_{11})+m_bm_s(C^h_{12}-C^h_0-C^h_{11})]\gamma^{\mu}P_R \\
& +[8m_b(C^f_{21}+C^f_{11})+4(C^h_{21}+6C^h_{11}+2C^h_0)]p^{\mu}_bP_L+[-8m_s(C^f_{11}+C^f_{23}) \\
& +m_s(2C^h_{11}+2C^h_0-4C^h_{23}-6C^h_{12})]p^{\mu}_bP_R+[8m_b(C^f_{23}+C^f_{11})+m_b(4C^h_{23} \\
& -2C^h_{11}-6C^h_{12}-2C^h_0)]p^{\mu}_{\bar{s}}P_L+[-8m_s(C^f_{11}+C^f_{22})-m_s(C^h_{22}+C^h_{12})]p^{\mu}_{\bar{s}}P_R\},
\end{aligned}$$

$$\begin{aligned}
\Gamma^{\mu}_{b\bar{s}\gamma}(W^{\pm}_{H}\omega^{\pm}) \;=\;& \frac{i}{16\pi^2}2eg^2(V_{Hd})^{*}_{ib}(V_{Hd})_{is} \\
& \times\{[m_s^2(C^i_{12}+m^2_{Hi}C^i_0)+m_b^2(C^j_0+C^j_{11})-m^2_{Hi}C^j_0]\gamma^{\mu}P_L+[m_bm_sC^i_0 \\
& +m_bm_sC^j_{12})]\gamma^{\mu}P_R+[-2m_sC^i_0]p^{\mu}_bP_R+[2m_bC^j_{12}]p^{\mu}_{\bar{s}}P_L\}.
\end{aligned}$$

$$\begin{aligned}
\Gamma^{\mu}_{b\bar{s}Z}(p_b,p_{\bar{s}}) \;=\;& \Gamma^{\mu}_{b\bar{s}Z}(\eta^0)+\Gamma^{\mu}_{b\bar{s}Z}(\omega^0)+\Gamma^{\mu}_{b\bar{s}Z}(\omega^{\pm})+\Gamma^{\mu}_{b\bar{s}Z}(A_H)+\Gamma^{\mu}_{b\bar{s}Z}(Z_H)+\Gamma^{\mu}_{b\bar{s}Z}(W^{\pm}_{H}) \\
& +\Gamma^{\mu}_{b\bar{s}Z}(W^{\pm}_{H}\omega^{\pm}),
\end{aligned}$$

$$\begin{aligned}
\Gamma^{\mu}_{b\bar{s}Z}(\eta^0) \;=\;& \frac{i}{16\pi^2}\frac{g}{c_w}(-\frac{1}{2}+\frac{1}{3}s_w^2)\frac{g'^2}{100M^2_{A_H}}(V_{Hd})^{*}_{ib}(V_{Hd})_{is}E, \\
& E=[\frac{m_b^2}{m_b^2-m_s^2}(m^2_{Hi}B_0(-p_b,m_{Hi},0)-m^2_{Hi}B_0(-p_{\bar{s}},m_{Hi},0) \\
& +m^2_{Hi}B_1(-p_b,m_{Hi},0)-m_s^2B_1(-p_{\bar{s}},m_{Hi},0))+\frac{m_s^2}{m_b^2-m_s^2}(m^2_{Hi}B_0(-p_b,m_{Hi},0) \\
& -m^2_{Hi}B_0(-p_{\bar{s}},m_{Hi},0)+m_b^2B_1(-p_b,m_{Hi},0)-m^2_{Hi}B_1(-p_{\bar{s}},m_{Hi},0)) \\
& +m^2_{Hi}(m_b^2(C^a_{21}+C^a_{11}+C^a_0)+m_s^2(C^a_{22}+C^a_{12}+C^a_0)+2p_b\cdot p_{\bar{s}}(C^a_{23}+C^a_{12}) \\
& +2C^a_{24}-m^2_{Hi}C^a_0)+m_s^2m_b^2(C^a_{11}-C^a_{12})]\gamma^{\mu}P_L+[\frac{m_bm_s}{m_b^2-m_s^2}(m^2_{Hi}(2B_0(-p_b,m_{Hi},0) \\
& -2B_0(-p_{\bar{s}},m_{Hi},0)+B_1(-p_b,m_{Hi},0)-B_1(-p_{\bar{s}},m_{Hi},0))+m_b^2B_1(-p_b,m_{Hi},0) \\
& -m_s^2B_1(-p_{\bar{s}},m_{Hi},0))+m^2_{Hi}m_bm_s(C^a_{11}-C^a_{12}+3C^a_0)+m_bm_s(m_b^2(C^a_{21}+C^a_{11}) \\
& +m_s^2(C^a_{22}+C^a_{12})+2p_b\cdot p_{\bar{s}}(C^a_{23}+C^a_{12})+2C^a_{24})]\gamma^{\mu}P_R+[(-2m^2_{Hi}m_b)(2C^a_{11} \\
& +C^a_{21}+C^a_0)+m_s^2m_b(C^a_{23}+C^a_{12})]p^{\mu}_bP_L+[2m^2_{Hi}m_s(C^a_{23}+C^a_{12}-C^a_{11}-C^a_0) \\
& -2m_sm_b^2(C^a_{21}+C^a_{11})]p^{\mu}_bP_R+[-2m^2_{Hi}m_b(2C^a_{12}+C^a_{23})+2m_bm_s^2(C^a_{12}+C^a_{22})]p^{\mu}_{\bar{s}}P_L \\
& +[2m^2_{Hi}m_sC^a_{22}-2m_sm_b^2(C^a_{12}+C^a_{23})]p^{\mu}_{\bar{s}}P_R,
\end{aligned}$$

$$\begin{aligned}
\Gamma^{\mu}_{b\bar{s}Z}(\omega^0) \;=\;& \frac{i}{16\pi^2}\frac{g}{c_w}(-\frac{1}{2}+\frac{1}{3}s_w^2)\frac{g^2}{4M^2_{Z_H}}(V_{Hd})^{*}_{ib}(V_{Hd})_{is}m^2_{Hi}F, \\
& F=E(C^a_{ij}\rightarrow\ C^b_{ij},C^a_0\rightarrow\ C^b_0),
\end{aligned}$$

$$
\begin{aligned}
\Gamma^{\mu}_{b\bar{s}Z}(\omega^{\pm}) \;=\; & \frac{i}{16\pi^2}\frac{g}{c_w}\frac{g^2}{2M^2_{W_H}}(V_{Hd})^*_{ib}(V_{Hd})_{is} \\
& \times\{[(-\frac{1}{2}+\frac{1}{3}s^2_w)(\frac{m_b^2}{m_b^2-m_s^2}(m^2_{Hi}B_0(-p_b,m_{Hi},0)-m^2_{Hi}B_0(-p_{\bar{s}},m_{Hi},0) \\
& +m^2_{Hi}B_1(-p_b,m_{Hi},0)-m_s^2B_1(-p_{\bar{s}},m_{Hi},0))+\frac{m_s^2}{m_b^2-m_s^2}(m^2_{Hi}B_0(-p_b,m_{Hi},0) \\
& -m^2_{Hi}B_0(-p_{\bar{s}},m_{Hi},0)+m_b^2B_1(-p_b,m_{Hi},0)-m^2_{Hi}B_1(-p_{\bar{s}},m_{Hi},0)) \\
& +(\frac{1}{2}-\frac{2}{3}s^2_w)(m^2_{Hi}(m_b^2(C^c_{21}+C^c_{11}+C^c_0)+m_s^2(C^c_{22}+C^c_{12}+C^c_0) \\
& +2p_b\cdot p_{\bar{s}}(C^c_{23}+C^c_{12})+2C^c_{24}-m^2_{Hi}C^c_0)+m_s^2m_b^2(C^c_{11}-C^c_{12}))-2m^2_{Hi}C^g_{24}]\gamma^{\mu}P_L \\
& +[(-\frac{1}{2}+\frac{1}{3}s^2_w)(\frac{m_bm_s}{m_b^2-m_s^2}(m^2_{Hi}(2B_0(-p_b,m_{Hi},0)-2B_0(-p_{\bar{s}},m_{Hi},0) \\
& +B_1(-p_b,m_{Hi},0)-B_1(-p_{\bar{s}},m_{Hi},0))+m_b^2B_1(-p_b,m_{Hi},0) \\
& -m_s^2B_1(-p_{\bar{s}},m_{Hi},0))+(\frac{1}{2}-\frac{2}{3}s^2_w)(m^2_{Hi}m_bm_s(C^c_{11}-C^c_{12}+3C^c_0) \\
& +m_bm_s(m_b^2(C^c_{21}+C^c_{11})+m_s^2(C^c_{22}+C^c_{12})+2p_b\cdot p_{\bar{s}}(C^c_{23}+C^c_{12})+2C^c_{24})) \\
& -2m_bm_sC^g_{24}]\gamma^{\mu}P_R+[(\frac{1}{2}-\frac{2}{3}s^2_w)(-2m^2_{Hi}m_b)(2C^c_{11}+C^c_{21}+C^c_0) \\
& +2m_s^2m_b(C^c_{23}+C^c_{12})+(m_bm_s^2(2C^g_{23}+C^g_{12})-m_{Hi}m_b(2C^g_{23}+C^g_{12}))]p^{\mu}_bP_L \\
& +[(\frac{1}{2}-\frac{2}{3}s^2_w)(2m^2_{Hi}m_s(C^c_{23}+C^c_{12}-C^c_{11}-C^c_0)-2m_sm_b^2(C^c_{21}+C^c_{11})) \\
& +m^2_{Hi}m_s(2C^g_{11}+C^g_0+2C^g_{23}+C^g_{12})-m_b^2m_s(3C^g_{11}+C^g_0+2C^g_{21})]p^{\mu}_bP_R \\
& +[(\frac{1}{2}-\frac{2}{3}s^2_w)(-2m^2_{Hi}m_b(2C^c_{12}+C^c_{23})+2m_bm_s^2(C^c_{12}+C^c_{22})) \\
& +m_bm_s^2(2C^g_{22}+C^g_{12})-m_{Hi}m_b(2C^g_{23}+C^g_{11})]p^{\mu}_{\bar{s}}P_L \\
& +[(\frac{1}{2}-\frac{2}{3}s^2_w)(2m^2_{Hi}m_sC^c_{22}-2m_sm_b^2(C^c_{12}+C^c_{23}))+m^2_{Hi}m_s(2C^c_{12} \\
& +C^c_0+2C^c_{22}+C^c_{12})-m_b^2m_s(2C^g_{12}+C^g_0+2C^g_{23}+C^g_{11})]p^{\mu}_{\bar{s}}P_R\},
\end{aligned}
$$

$$
\begin{aligned}
\Gamma^{\mu}_{b\bar{s}Z}(A_H) \; = \; & \frac{i}{16\pi^2}\frac{g}{c_w}\frac{g'^2}{50}V_{Hd})^*_{ib}(V_{Hd})_{is}G, \\
& G = (-\frac{1}{2}+\frac{1}{3}s_w^2)[\frac{m_b^2}{m_b^2-m_s^2}B_1(-p_b, m_{Hi}, M_{A_H}) \\
& -\frac{m_s^2}{m_b^2-m_s^2}B_1(-p_{\bar{s}}, m_{Hi}, M_{A_H}) + m_b^2(C^d_{21}+C^d_{11}) + m_s^2(C^d_{12}+C^d_{22}) \\
& +2p_b\cdot p_{\bar{s}}(C^d_{11}+C^d_{23}) + 2C^d_{24} - m^2_{Hi}C^d_0]\gamma^\mu P_L \\
& +\frac{1}{3}s_w^2[\frac{m_bm_s}{m_b^2-m_s^2}(B_1(-p_b, m_{Hi}, M_{A_H}) - B_1(-p_{\bar{s}}, m_{Hi}, M_{A_H})) \\
& +m_bm_s(C^d_{12}-C^d_{11})]\gamma^\mu P_R + (-\frac{1}{2}+\frac{1}{3}s_w^2)[-2m_b(C^d_{21}+C^d_{11})]p_b^\mu P_L \\
& +(-\frac{1}{2}+\frac{1}{3}s_w^2)[2m_s(C^d_{11}+C^d_{23})]p_b^\mu P_R + (-\frac{1}{2}+\frac{1}{3}s_w^2)[-2m_b(C^d_{23} \\
& +C^d_{11})]p_{\bar{s}}^\mu P_L + (-\frac{1}{2}+\frac{1}{3}s_w^2)[2m_s(C^d_{11}+C^d_{22})]p_{\bar{s}}^\mu P_R,
\end{aligned}
$$

$$
\begin{aligned}
\Gamma^{\mu}_{b\bar{s}Z}(Z_H) \; = \; & \frac{i}{32\pi^2}\frac{g^3}{c_w}V_{Hd})^*_{ib}(V_{Hd})_{is}H, \\
& H = G(C^d_{ij} \rightarrow \; C^e_{ij}, C^d_0 \rightarrow \; C^e_0),
\end{aligned}
$$

$$
\begin{aligned}
\Gamma^{\mu}_{b\bar{s}Z}(W_H^{\pm}) \; = \; & \frac{i}{16\pi^2}\frac{g^3}{c_w}(V_{Hd})^*_{ib}(V_{Hd})_{is} \\
& \times\{(-\frac{1}{2}+\frac{1}{3}s_w^2)[\frac{2m_b^2}{m_b^2-m_s^2}B_1(-p_b, m_{Hi}, M_{W_H}) \\
& -\frac{2m_s^2}{m_b^2-m_s^2}B_1(-p_{\bar{s}}, m_{Hi}, M_{W_H}) - 4m_b^2(C^f_{21}+C^f_{11}) - 4m_s^2(C^f_{22}+C^f_{12}) \\
& -8p_b\cdot p_{\bar{s}}(C^f_{11}+C^f_{23}) - 8C^f_{24} + 4m^2_{Hi}C^f_0 + 4C^h_{24} + 2B_0(-p_{\bar{s}}, m_{Hi}, M_{W_H}) \\
& +2m^2_{WH}C^h_0 + m_b^2(3C^h_{11}+C^h_0) + m_s^2C^h_{12} + 4p_b\cdot p_{\bar{s}}(C^h_0+C^h_{11})]\gamma^\mu P_L \\
& +[\frac{1}{3}s_w^2\frac{m_bm_s}{m_b^2-m_s^2}(B_1(-p_t, m_{Hi}, M_{W_H}) - B_1(-p_{\bar{s}}, m_{Hi}, M_{W_H})) \\
& -(-\frac{1}{2}+\frac{1}{3}s_w^2)m_bm_s(C^f_{12}-C^f_{11}) + (-\frac{1}{2}+\frac{1}{3}s_w^2)m_bm_s(C^h_{12} \\
& -C^h_0-C^h_{11})]\gamma^\mu P_R + (-\frac{1}{2}+\frac{1}{3}s_w^2)[8m_b(C^f_{21}+C^f_{11}) + 4(C^h_{21}+6C^h_{11} \\
& +2C^h_0)]p_b^\mu P_L + (-\frac{1}{2}+\frac{1}{3}s_w^2)[-8m_s(C^f_{11}+C^f_{23}) + m_s(2C^h_{11}+2C^h_0 \\
& -4C^h_{23}-6C^h_{12})]p_b^\mu P_R + (-\frac{1}{2}+\frac{1}{3}s_w^2)[8m_b(C^f_{23}+C^f_{11}) + m_b(4C^h_{23} \\
& -2C^h_{11}-6C^h_{12}-2C^h_0)]p_{\bar{s}}^\mu P_L + (-\frac{1}{2}+\frac{1}{3}s_w^2)[-8m_s(C^f_{11}+C^f_{22}) \\
& -m_s(C^h_{22}+C^h_{12})]p_{\bar{s}}^\mu P_R\},
\end{aligned}
$$

$$\begin{aligned}\Gamma^{\mu}_{b\bar{s}Z}(W^{\pm}_{H}\omega^{\pm}) &= \frac{ig^3}{8\pi^2}c_w(V_{Hd})^*_{ib}(V_{Hd})_{is} \\ &\times\{[m_s^2(C^i_{12}+m^2_{Hi}C^i_0)+m_b^2(C^j_0+C^j_{11})-m^2_{Hi}C^j_0]\gamma^{\mu}P_L+[m_bm_sC^i_0 \\ &+m_bm_sC^j_{12})]\gamma^{\mu}P_R+[-2m_sC^i_0]p^{\mu}_bP_R+[2m_bC^j_{12}]p^{\mu}_{\bar{s}}P_L\},\end{aligned}$$

The three-point standard functions $C_0,\ C_{ij}$ are defined as

$$\begin{aligned}C^a_{ij} &= C^a_{ij}(-p_b,-p_{\bar{s}},m_{Hi},0,m_{Hi}), \\ C^b_{ij} &= C^b_{ij}(-p_b,-p_{\bar{s}},m_{Hi},0,m_{Hi}), \\ C^c_{ij} &= C^c_{ij}(-p_b,-p_{\bar{s}},m_{Hi},0,m_{Hi}), \\ C^d_{ij} &= C^d_{ij}(-p_b,-p_{\bar{s}},m_{Hi},M_{A_H},m_{Hi}), \\ C^e_{ij} &= C^e_{ij}(-p_b,-p_{\bar{s}},m_{Hi},M_{Z_H},m_{Hi}), \\ C^f_{ij} &= C^f_{ij}(-p_b,-p_{\bar{s}},m_{Hi},M_{W_H},m_{Hi}), \\ C^g_{ij} &= C^g_{ij}(-p_b,-p_{\bar{s}},0,m_{Hi},0), \\ C^h_{ij} &= C^h_{ij}(-p_b,-p_{\bar{s}},M_{W_H},m_{Hi},M_{W_H}), \\ C^i_{ij} &= C^i_{ij}(-p_b,-p_{\bar{s}},M_{W_H},m_{Hi},0), \\ C^j_{ij} &= C^j_{ij}(-p_b,-p_{\bar{s}},0,m_{Hi},M_{W_H}).\end{aligned}$$

Appendix B: The definitions of the standard functions

The definitions of the two-point and three-point standard functions have been given in Ref.[22], here we only show their definitions and explicit expressions related to our calculation.

The functions $A_0,\ B_0,\ B_\mu,\ C_0,\ C_\mu,\ C_{\mu\nu}$ are defined as

$$\begin{aligned}
&\frac{i}{16\pi^2}A_0(m) = \mu^{2\epsilon}\int\frac{d^nq}{(2\pi)^n}\frac{1}{q^2-m^2},\\
&\frac{i}{16\pi^2}B_0,\ B_\mu(p,m_1,m_2) = \mu^{2\epsilon}\int\frac{d^nq}{(2\pi)^n}\frac{1, q_\mu}{(q^2-m_1^2)[(q+p)^2-m_2^2]},\\
&\frac{i}{16\pi^2}C_0, C_\mu, C_{\mu\nu}(p,k,m_1,m_2,m_3) =\\
&\mu^{2\epsilon}\int\frac{d^nq}{(2\pi)^n}\frac{1, q_\mu, q_{\mu\nu}}{(q^2-m_1^2)[(q+p)^2-m_2^2][(q+p+k)^2-m_3^2]}.
\end{aligned}$$

The explicit expressions of basic functions $A_0,\ B_n(n=0,1),\ C_0$ are

$$\begin{aligned}
A_0(m) &= m^2[\Delta - ln\frac{m^2}{\mu^2}+1],\\
B_n(p,m_1,m_2) &= [\frac{\Delta}{n+1}-\int_0^1 dx\ x^n ln\frac{x^2p^2-x(p^2+m_1^2-m_2^2)+m_1^2}{\mu^2}](-1)^n,\\
C_0(p,k,m_1,m_2,m_3) &= \int_0^1 dx\int_0^x dy[ax^2+by^2+cxy+dx+ey+f]^{-1},
\end{aligned}$$

with

$$\begin{aligned}
&a=-k^2,\quad b=-p^2,\quad c=-2p.k,\quad d=-m_2^2+m_3^2+k^2,\\
&e=-m_1^2+m_2^2+p^2+2p.k,\qquad f=-m_3^2.
\end{aligned}$$

The definition of the divergent term Δ is

$$\Delta=\frac{1}{\epsilon}-\gamma+ln4\pi,\qquad \epsilon=2-\frac{n}{2}.$$

The functions $B_\mu,\ C_\mu, C_{\mu\nu}$ can be obtained based on the following relations

$$\begin{aligned}
B_\mu(p,m_1,m_2) &= p_\mu B_1(p,m_1,m_2),\\
C_\mu(p,k,m_1,m_2,m_3) &= p_\mu C_{11}+k_\mu C_{12},\\
C_{\mu\nu}(p,k,m_1,m_2,m_3) &= p_{1\mu}p_{1\nu}C_{21}+p_{2\mu}p_{2\nu}C_{22}+(p_{1\mu}p_{2\nu}+p_{1\nu}p_{2\mu})C_{23}+g_{\mu\nu}C_{24},
\end{aligned}$$

and the function C_{24} is

$$C_{24}(p,k,m_1,m_2,m_3) = \frac{\Delta}{4}+\frac{1}{4}[1-\bar{B}_0(k,m_2,m_3)+2m_1^2C_0+f_1C_{11}+f_2C_{12}],$$

with

$$f_1=m_1^2-m_2^2+p^2,\quad f_2=m_2^2-m_3^2+(p+k)^2-p^2.$$

The explicit expressions of other three-point functions C_{ij} can be found in Ref.[22].

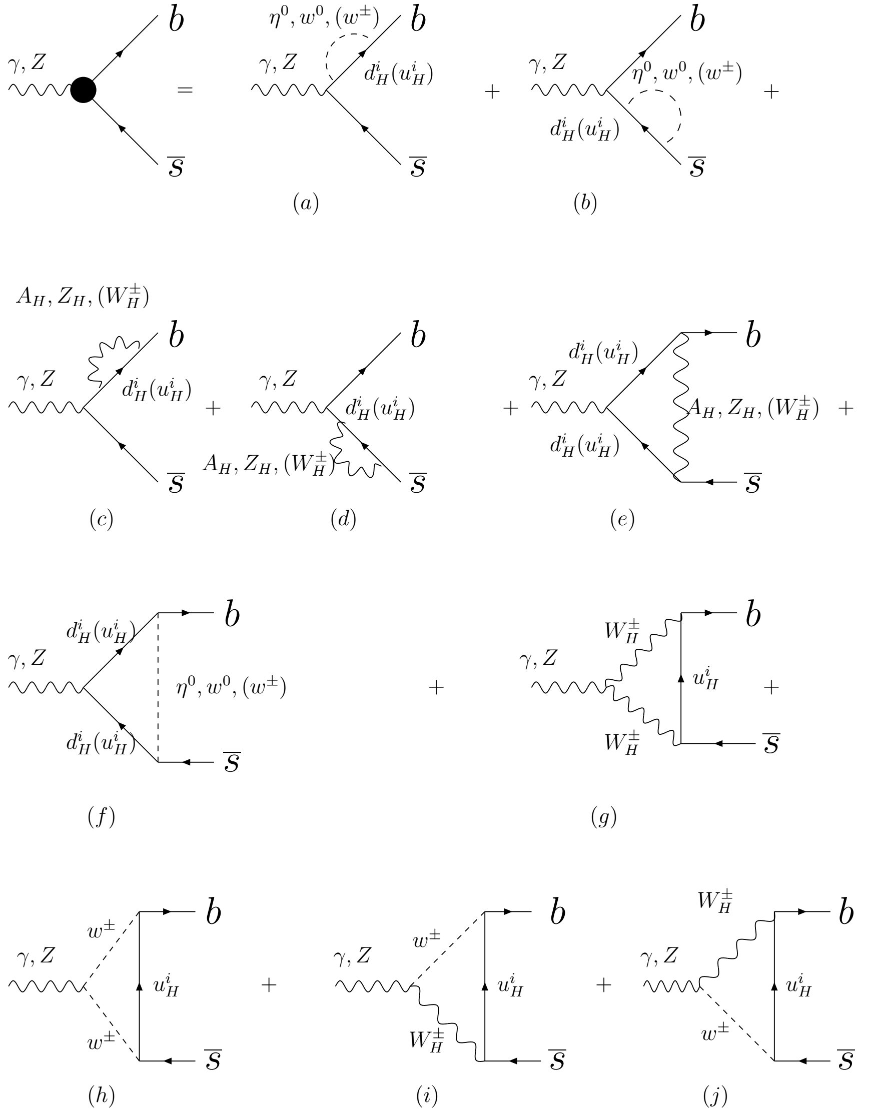

FIG. 1: The Feynman diagrams of the one-loop contributions of the LHT model to the couplings $b\bar{s}Z(\gamma)$.

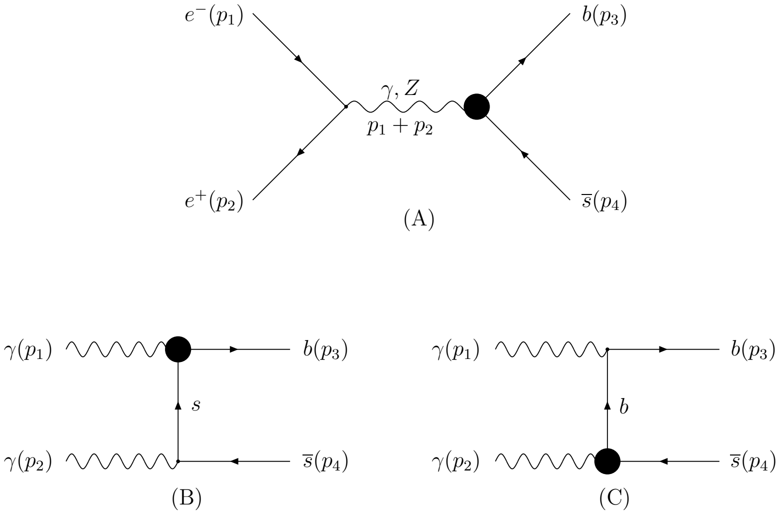

FIG. 2: The Feynman diagrams of the processes $e^+e^-(\gamma\gamma) \to b\bar{s}$ in the LHT model.

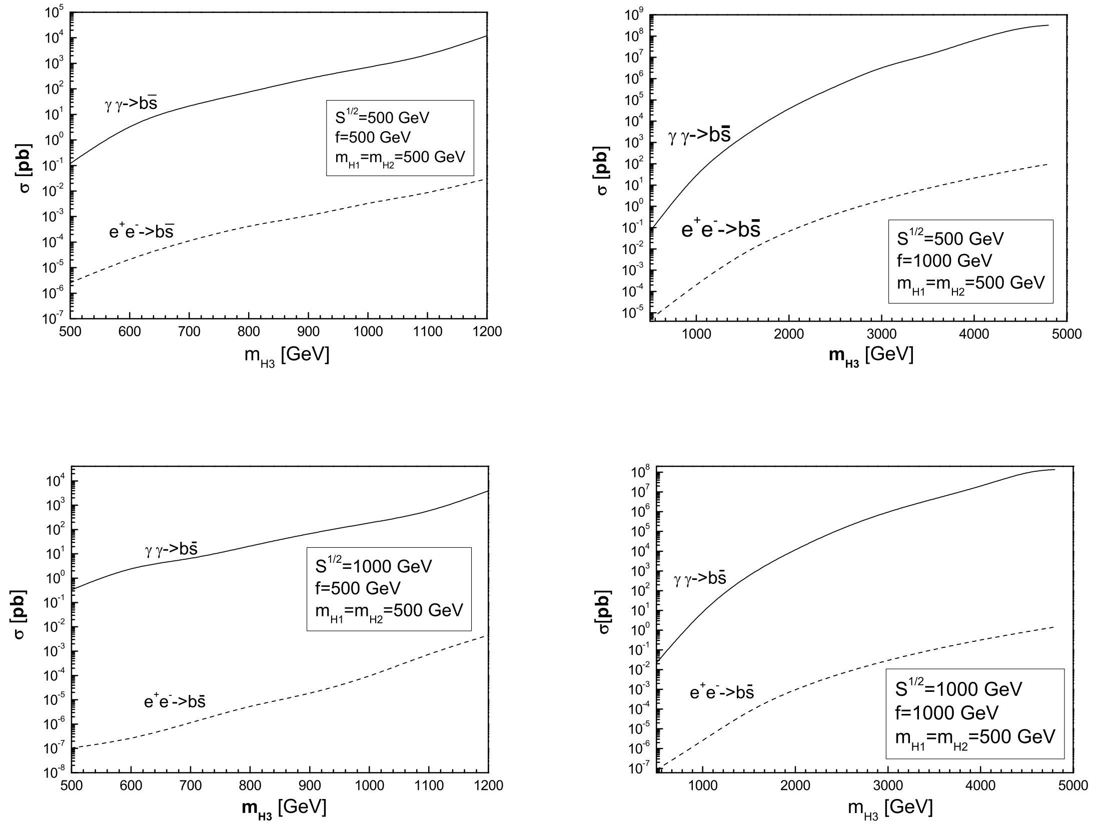

FIG. 3: The cross sections of the processes $e^+e^-(\gamma\gamma) \rightarrow b\bar{s}$ in the LHT model for Case I, as a function of M_{H_3}.

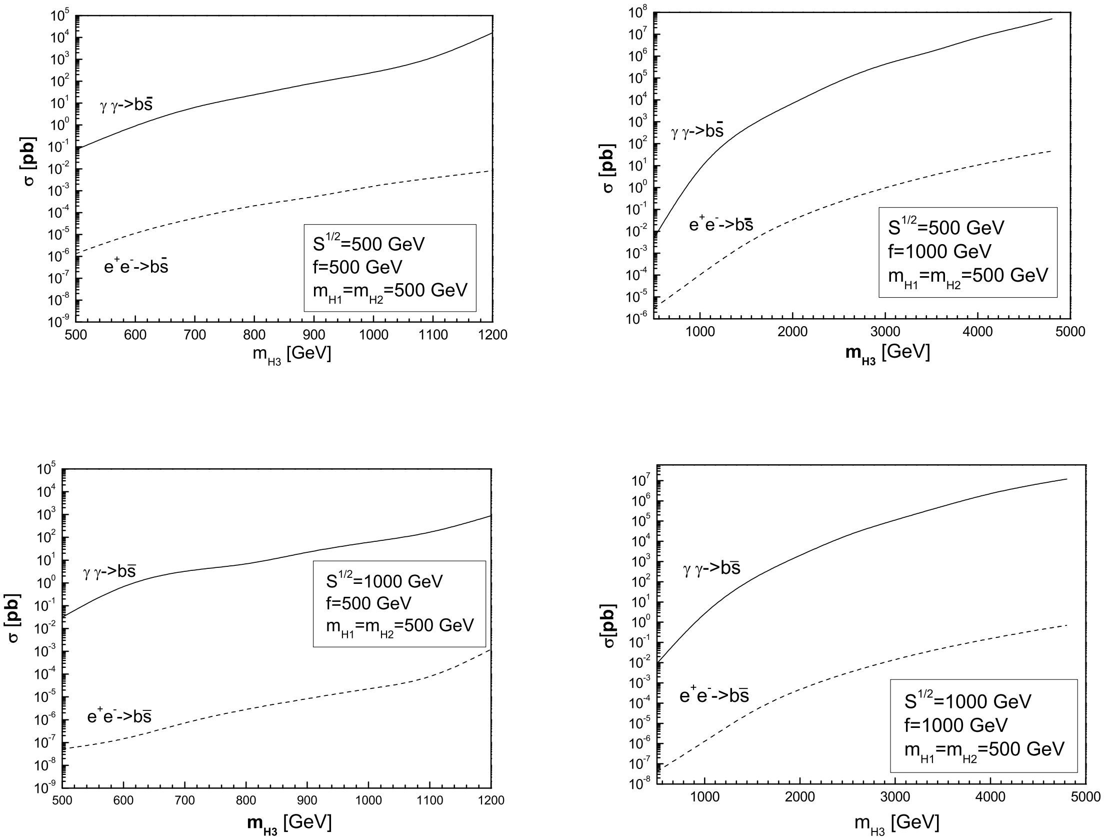

FIG. 4: The cross sections of the processes $e^{+}e^{-}(\gamma\gamma) \rightarrow b\bar{s}$ in the LHT model for Case II(1) , as a function of M_{H_3}.

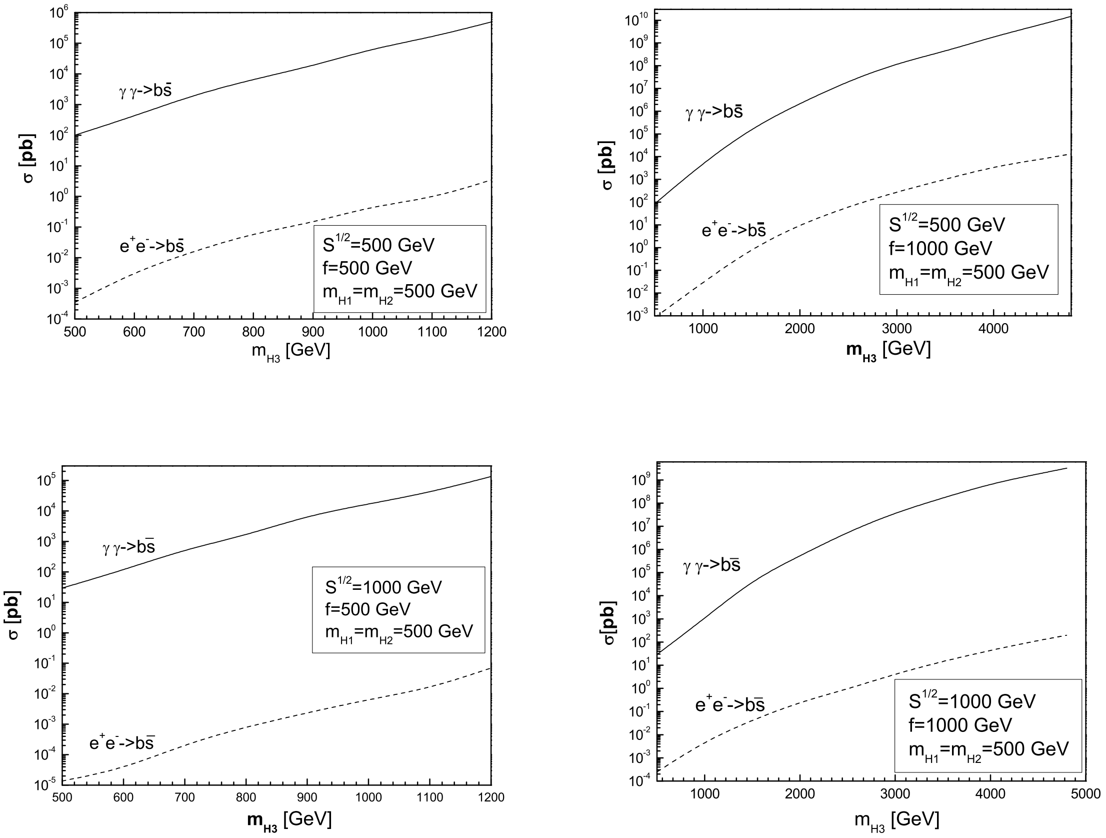

FIG. 5: The cross sections of the processes $e^+e^-(\gamma\gamma) \rightarrow b\bar{s}$ in the LHT model for Case II(2) , as a function of M_{H_3}.

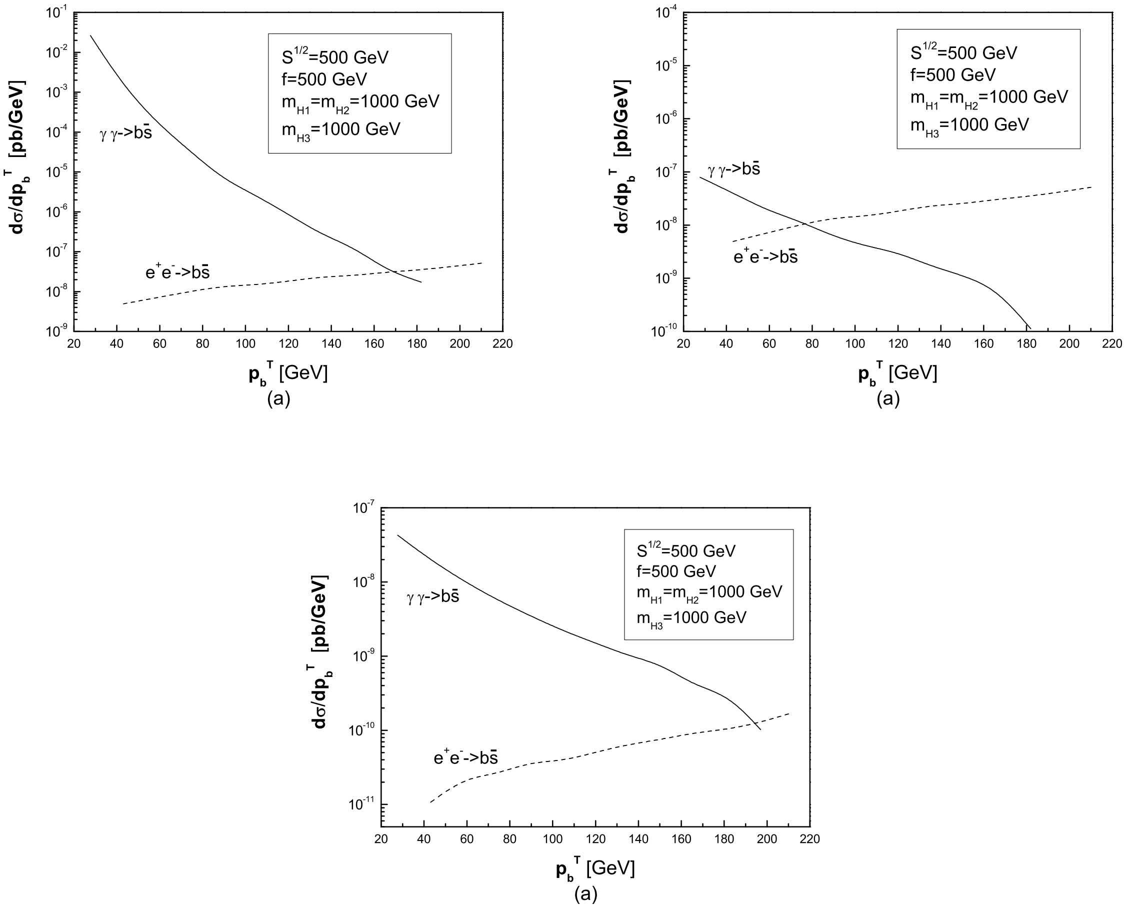

FIG. 6: The transverse momentum distributions of the top quark for the processes $e^+e^-(\gamma\gamma) \rightarrow b\bar{s}$ in the LHT model. The up-left diagram is for Case I, the up-right diagram is for Case II(1) and the down diagram is for Case II(2).